2256 *Biochemistry* **2010,** *49,* 2256–2268
DOI: 10.1021/bi902115v

BIOCHEMISTRY
including biophysical chemistry & molecular biology
Article

Polcalcin Divalent Ion-Binding Behavior and Thermal Stability: Comparison of Bet v 4, Bra n 1, and Bra n 2 to Phl p 7[†]

Michael T. Henzl,* Meredith E. Davis, and Anmin Tan

Department of Biochemistry, University of Missouri, Columbia, Missouri 65211

Received December 10, 2009; Revised Manuscript Received February 4, 2010

ABSTRACT: Polcalcins are pollen-specific proteins containing two EF-hands. Atypically, the C-terminal EF-hand binding loop in Phl p 7 (from timothy grass) harbors five, rather than four, anionic side chains, due to replacement of the consensus serine at $-x$ by aspartate. This arrangement has been shown to heighten parvalbumin Ca^{2+} affinity. To determine whether Phl p 7 likewise exhibits anomalous divalent ion affinity, we have also characterized Bra n 1 and Bra n 2 (both from rapeseed) and Bet v 4 (from birch tree). Relative to Phl p 7, they exhibit N-terminal extensions of one, five, and seven residues, respectively. Interestingly, the divalent ion affinity of Phl p 7 is unexceptional. For example, at -17.84 ± 0.13 kcal mol^{-1}, the overall standard free energy for Ca^{2+} binding falls within the range observed for the other three proteins (-17.30 ± 0.10 to -18.15 ± 0.10 kcal mol^{-1}). In further contrast to parvalbumin, replacement of the $-x$ aspartate, via the D55S mutation, actually increases the overall Ca^{2+} affinity of Phl p 7, to -18.17 ± 0.13 kcal mol^{-1}. Ca^{2+}-free Phl p 7 exhibits uncharacteristic thermal stability. Whereas wild-type Phl p 7 and the D55S variant denature at 77.3 and 78.0 °C, respectively, the other three polcalcins unfold between 56.1 and 57.9 °C. This stability reflects a low denaturational heat capacity increment. Phl p 7 and Phl p 7 D55S exhibit ΔC_p values of 0.34 and 0.32 kcal mol^{-1} K^{-1}, respectively. The corresponding values for the other three polcalcins range from 0.66 to 0.95 kcal mol^{-1} K^{-1}.

Polcalcins are small, EF-hand proteins expressed in the anthers and pollen of flowering plants (*1*−*4*). Enrichment of the proteins at the tips of growing pollen tubes implies a role for polcalcins in regulating the direction of pollen tube growth (*5*). Anecdotal spectroscopic evidence for several of the proteins suggested that they undergo a Ca^{2+}-dependent conformational change (*1*, *2*, *5*−*7*) which would be consistent with an explicit regulatory function. However, the putative biological targets are presently unidentified. Interestingly, the polcalcins are potent plant allergens, and the allergenicity is primarily associated with the Ca^{2+}-bound form of the protein (*1*, *6*, *8*).

The 30-residue EF-hand motif includes a central metal ion-binding loop flanked by short helical segments (*9*−*11*). The spatial arrangement of these structural elements can be mimicked with the fingers of the right hand (*12*). Within the loop, the ligands to the bound metal ion, positioned at the vertices of an octahedron, are indexed by a set of Cartesian axes (*13*).

We recently studied the divalent ion-binding behavior of Phl p 7, expressed by timothy grass (*14*). Addition of the Ca^{2+}-bound protein, but not the Ca^{2+}-free protein, to a solution of ANS[1] yields a substantial increase in fluorescence emission, implying that Ca^{2+} binding provokes exposure of apolar surface. Consistent with that observation, Phl p 7 binds Ca^{2+} with macroscopic positive cooperativity. By contrast, addition of Phl p 7 to ANS in the presence of Mg^{2+} has no impact on the dye emission, and Mg^{2+} binding is correspondingly noncooperative.

Curiosity in Phl p 7 was originally kindled by the recognition that EF-hand 2 harbors five anionic residues: aspartates at $+x$, $+y$, $+z$, $-x$ and glutamate at $-z$. This constellation of ligands, apparently unique to Phl p 7, substantially increases divalent ion affinity when introduced into the CD or EF sites of either rat α- or β-parvalbumin (*15*, *16*). To determine whether the additional carboxylate likewise confers elevated affinity to Phl p 7, we have characterized three additional polcalcin isoforms: Bra n 1 and Bra n 2 (both from rapeseed, *Brassica napus*) and Bet v 4 (from birch tree, *Betula verrucosa*). Although highly conserved, polcalcin sequences differ at the N-terminus. Relative to Phl p 7, perhaps the smallest polcalcin, Bra n 1, Bra n 2, and Bet v 4 display extensions of one, five, and seven residues, respectively (Figure 1A). We have also examined the impact of replacing D55 in Phl p 7 with the polcalcin consensus residue, serine.

The previous study of Phl p 7 included an evaluation of the apoprotein conformational stability by DSC. The protein was observed to denature at 78 °C. By contrast, the T_m previously reported for Bet v 4 was just 45 °C. In order to determine whether Phl p 7 is truly exceptional in this regard, we have also examined the stabilities of Bet v 4, Bra n 1, Bra n 2, and the D55S variant of Phl p 7.

MATERIALS AND METHODS

Materials. NaCl, Hepes, $CaCl_2 \cdot 2H_2O$, $MgCl_2 \cdot 2H_2O$, NaH_2PO_4, EGTA, NTA, $Na_2EDTA \cdot 2H_2O$, lysozyme, Spectrapor 1

[†]This work was supported by NSF Award MCB0543476 (to M.T.H.).
*To whom correspondence should be addressed. Tel: 573-882-7485. Fax: 573-884-4812. E-mail: henzlm@missouri.edu.

[1]Abbreviations: ANS, 8-anilinonaphthalene-1-sulfonate; CD, circular dichroism; CD site, the metal ion-binding site in parvalbumin flanked by the C and D helical segments; EF site, the metal ion-binding site flanked by the E and F helical segments; DMPC, dimyristoylphosphatidylcholine; DPPC, dipalmitoylphosphatidylcholine; DSC, differential scanning calorimetry; DSPC, distearoylphosphatidylcholine; EDTA, ethylenediaminetetraacetic acid; EGTA, ethylene glycol bis(β-aminoethyl ether)-*N*,*N*,*N*′,*N*′-tetraacetic acid; HBS, Hepes-buffered saline; Hepes, 4-(2-hydroxyethyl)-1-piperazineethanesulfonic acid; IPTG, isopropyl β-D-thiogalactopyranoside; ITC, isothermal titration calorimetry; LB, Luria−Bertani; NaP_i, sodium phosphate; NTA, nitrilotriacetic acid; PAGE, polyacrylamide gel electrophoresis, PBS, phosphate-buffered saline; PV, parvalbumin; THP, tris(hydroxypropyl)phosphine.

 Published on Web 02/09/2010

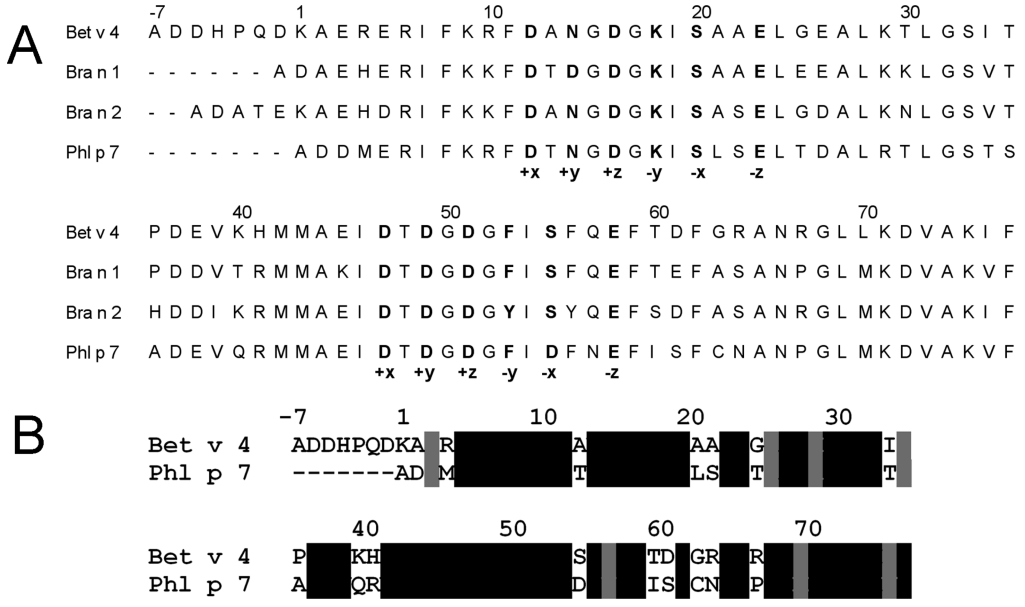

FIGURE 1: (A) Primary structures of Bet v 4, Bra n 1, Bra n 2, and Phl p 7. (B) Comparison of the Bet v 4 and Phl p 7 amino acid sequences. Black denotes residues that are identical in the two proteins; gray denotes highly conservative sequence substitutions. The numbering scheme employed in panels A and B is based on Phl p 7, the shortest of the four isoforms.

dialysis tubing (MWCO 6000−8000), *N*,*N*′-methylenebis(acrylamide), and acrylamide were purchased from Fisher Scientific Co. LB agar, LB broth, and ampicillin were obtained from Research Products International. IPTG and DTT were purchased from Gold Biotechnology. DEAE-Sepharose, Sephadex G-75, THP, and ANS were obtained from Sigma-Aldrich Co.

Protein Expression and Purification. The coding sequences of Bet v 4, Bra n 1, and Bra n 2, optimized for expression in *Escherichia coli*, were synthesized by GenScript Corp. (Piscataway, NJ) and subcloned into pET11a (Novagen) between the *Nde*I and *Bam*HI sites. Following transformation, *E. coli* BL21(DE3) harboring the appropriate construct were cultured at 37 °C in LB broth (Miller) supplemented with ampicillin (100 μg/mL). When the turbidity at 600 nm reached 0.6, expression was induced with IPTG (0.25 mM). After an additional 16 h, the bacteria were harvested and resuspended in 5 volumes of 20 mM Hepes, pH 7.4. A similar protocol was employed for the isolation of all three proteins. Lysis was achieved by passing the cell suspension through a French pressure cell, following lysozyme treatment (15 min, 37 °C, 5 mg of lysozyme/g of cell paste). Removal of cell debris (30 min at 27000*g*) and subsequent purification steps were performed at 4 °C.

The clarified lysate was diluted with an equal volume of cold deionized water and loaded onto DEAE-Sepharose (4 mL/g of cell paste), preequilibrated with 20 mM Hepes, pH 7.4. The column was eluted, at 0.5 mL/min, with a NaCl gradient (0−0.6 M, 10 column bed volumes). Fractions containing the protein of interest were identified by nondenaturing PAGE, combined, concentrated (to 6 mL), and loaded onto Sephadex G-75 (3.0 cm × 90 cm), preequilibrated with 0.15 M NaCl and 0.025 M Hepes, pH 7.4 (Hepes-buffered saline, HBS). Lacking tryptophan (Bet v 4 and Bra n 1 lack tyrosine as well) the polcalcins have characteristic absorption spectra that permit their elution from the column to be monitored by UV absorbance measurements.

The material collected from the G-75 column was subjected to a second round of anion-exchange chromatography, conducted in the presence of EDTA. Following extensive dialysis against 20 mM Hepes and 1 mM EDTA, pH 7.4, the preparation was loaded onto DEAE-Sepharose that had been equilibrated with the same buffer and then eluted with a NaCl gradient. The purity of the preparations exceeded 95% in all cases.

The D55S mutation was introduced into the Phl p 7 coding sequence, in pET11b, with the QuikChange site-directed mutagenesis kit (Stratagene), employing oligonucleotide primers from Integrated DNA Technologies, Inc. (Coralville, IA). The fidelity of the mutated coding sequence was confirmed by automated DNA sequencing. The purification protocol for the D55S variant was identical to that described previously for the wild-type protein.

Protein concentrations were estimated spectrophotometrically, employing molar extinction coefficients of 1400 M^{-1} cm^{-1} (at 257 nm) for Bet v 4, Bra n 1, Phl p 7, and Phl p 7 D55S and 3000 M^{-1} cm^{-1} (at 274 nm) for Bra n 2.

Fluorescence Spectroscopy. The emission spectrum of ANS was examined in the absence and presence of the various polcalcin isoforms using an SLM-Aminco 8100 fluorometer, modified for photon counting. Emission data were collected at 1 nm intervals between 380 and 600 nm, averaging for 1 s at each point, with excitation at 365 nm. A nominal 4 nm bandpass was employed for both excitation and emission channels.

A nominal 1.0 mM ANS solution was prepared in Hepes-buffered saline and standardized spectrophotometrically (ε = 4950 M^{-1} cm^{-1}) (*17*). This stock solution was diluted to 10 μM in HBS containing either 200 μM Ca^{2+}, 50 mM EDTA, or 2.0 mM Mg^{2+} and 1.0 mM EGTA. After collecting the spectrum of the ANS alone, additions of Ca^{2+}-free polcalcin were made to yield final concentrations of 25, 50, 75, and 100 μM protein. Data were collected at 25 °C in a 1.0 cm quartz cuvette.

Chemical Denaturation. Samples (2.0 mL, 50 μM) of Ca^{2+}-free protein, in PBS/EDTA, were titrated with urea while monitoring ellipticity at 240 nm in an Aviv 62DS circular dichroism spectrometer. Aliquots of denaturant solution were added with an automated titrator (Hamilton Microlab 500), operated in constant volume mode. Following each injection of titrant, the sample was allowed to equilibrate with stirring for 120 s prior to data acquisition (30 s).

To prepare the nominal 10.0 M titrant solution, 60.07 g of urea was transferred to a 100 mL volumetric flask, along with 10.0 mL of 10× PBS solution. Following addition of sufficient water to effect dissolution of the urea and equilibration to room temperature, the solution was diluted to 100 mL, and the pH was readjusted to 7.40. The actual urea concentration was determined by refractometry, using the relationship $M = 117.66(\Delta\eta) + 29.753(\Delta\eta)^2 + 185.56(\Delta\eta)^3$ (*18*), where $\Delta\eta$ is the difference between the refractive index of the urea solution and that of the buffer.

Sedimentation Equilibrium. Analyses were conducted at 20 °C in a Beckman XL-I analytical ultracentrifuge. The Ca^{2+}-free proteins were produced by extensive dialysis against HBS containing 5.0 mM EDTA. The Ca^{2+}-bound proteins were dialyzed extensively vs HBS containing 100 μM Ca^{2+} prior to analysis. THP (2.0 mM) was also included in the buffer used for dialysis of Phl p 7 and Phl p 7 D55S. Sedimentation was conducted in six-sector charcoal-Epon centerpieces, permitting examination of three loading concentrations in a single cell. Radial solute distributions, monitored at 257 nm (Bra n 1, Bet v 4, Phl p 7 D55S) or 274 nm (Bra n 2), were collected at 1 h intervals until successive data sets were indistinguishable. Typically, 10 absorbance readings were averaged at each radial position. Data were collected at 20000, 30000, and 40000 rpm.

The absorbance profiles for all nine sample−solvent pairs were subjected to global weighted nonlinear least-squares analysis in Origin v.7.5 (OriginLab). The data were satisfactorily accommodated by an equation describing the radial distribution of a single ideal species:

$$a = a_o \exp\left[\frac{M\omega^2(1-\bar{v}\rho)}{2RT}(r^2 - r_o{}^2)\right] + \mathrm{bl} \qquad (1)$$

where a is the absorbance at radial position r, a_o is the absorbance at an arbitrary reference position r_o, M is the molecular weight, ω is the angular velocity, $\bar{v}$ is the partial specific volume, ρ is the solution density, R is the gas constant, T is the absolute temperature, and bl is a baseline offset to account for optical mismatch between the sample and solvent sectors. The partial specific volume was set to 0.71 cm^3/g, based on the amino acid compositions of the proteins (*19*), and the solvent density was measured with an Anton-Paar DMA 5000 densimeter.

Isothermal Titration Calorimetry (*ITC*). Prior to analysis, residual Ca^{2+} was removed from the protein preparations by treatment with EDTA-derivatized agarose (*20*, *21*), as described previously for Phl p 7 (*14*). The resulting material contained less than 0.02 mol equiv of Ca^{2+}, as determined by atomic absorption spectrometry. Similarly treated buffer contained undetectable levels of Ca^{2+} (< 0.2 μM).

ITC experiments were conducted in Hepes-buffered saline, at 25 °C, employing a VP-ITC calorimeter (MicroCal, LLC). Following thermal equilibration, titrant was added to the 1.41 mL sample at 240 s intervals. All titrations included a 2 μL preaddition, the heat from which was neglected during data analysis. Ca^{2+} and Mg^{2+} concentrations were determined by titrating standard EDTA solutions, prepared from analytical reagent grade $Na_2EDTA \cdot 2H_2O$.

Samples of protein (typically 50−60 μM) were titrated with Ca^{2+} in the presence and absence of competitive chelators (EDTA, EGTA, and NTA) or Mg^{2+} and with Mg^{2+} in the presence and absence of EDTA. Following integration of the raw data, using software supplied with the instrument, the resulting composite data set, which typically included 11 experiments, was subjected to simultaneous least-squares minimization. This global approach yields estimates of the binding constants and enthalpies for Ca^{2+} and Mg^{2+} that are consistent with all of the titrations.

After identifying the optimal parameter values and the lowest chi square, $\chi^2(\mathrm{min})$, confidence limits are estimated by incrementing the parameter of interest, fixing its value, and repeating the least-squares minimization, allowing the remaining parameters to vary. This procedure is repeated until the chi square value, $\chi^2(\mathrm{par})$, exceeds a specified threshold, given by

$$\chi^2(\mathrm{par}) = \left(1 + \frac{p}{\nu}F(p, \nu, P)\right)(\chi^2(\mathrm{min})) \qquad (2)$$

In eq 2, p is the number of fitting parameters, ν the degrees of freedom, P the probability that the increase in χ^2 could be the result of random errors (0.32 for the 68% confidence limit), and $F(p, \nu, P)$ the corresponding F statistic (*22*). After determining the upper limit, the parameter value is decremented from its optimal value until $\chi^2(\mathrm{par})$ again exceeded the specified threshold. More detailed discussions of the data analysis have been presented elsewhere (*23*−*25*).

As observed for Phl p 7, the binding of Ca^{2+} to Bet v 4, Bra n 1, and Bra n 2 occurs with positive cooperativity, necessitating the use of macroscopic binding constants. The equations used to treat these data have been presented elsewhere (*14*). In our previous analysis of Phl p 7, we set the enthalpy change associated with the formation of the mixed $Ca^{2+}-Mg^{2+}$ species equal to the sum of the enthalpies associated with the first Ca^{2+}-binding event and the second Mg^{2+}-binding event. In the analyses described here, we allowed this enthalpy value to float. In every case, the improvement in chi square justified inclusion of the additional fitting parameter. For example, the reduced chi square value associated with fitting the Phl p 7 data decreased from 5.14 to 3.05, a ratio of 1.69. For a data set with more than 120 degrees of freedom, the ratio of the two values would only need to exceed 1.09 to be judged significant at the 68% confidence limit or 1.53 to be judged significant at the 99% confidence limit.

Differential Scanning Calorimetry (*DSC*). DSC was performed in a modified nano-DSC (Calorimetry Sciences Corp.) equipped with cylindrical hastalloy cells, having nominal volumes of 0.32 mL. Temperature calibration was verified with DMPC, DPPC, and DSPC, and the accuracy of the differential power measurements was verified with internally generated electrical calibration pulses.

Samples were dialyzed extensively against 0.15 M NaCl, 0.01 M NaP_i, and 0.005 M EDTA, pH 7.4 (PBS/EDTA), which then served as the reference. Sample and reference solutions were briefly degassed under vacuum prior to loading. A scan rate of 60°/h was employed for all experiments. Each of the proteins included in the study exhibits an endotherm on rescan, indicating reversible denaturation. A baseline, obtained with sample and reference cells filled with buffer, was subtracted from the protein data prior to analysis. Data collected at four protein concentrations were subjected to global nonlinear least-squares analysis to extract estimates of T_m, ΔH_{cal}, ΔH_{vH}, and ΔC_p, as described elsewhere (*26*).

The posttransition baselines of Phl p 7 and Phl p 7 D55S include an additional exothermic contribution not observed with the other three proteins included in the study. This signal might reflect the onset of aggregation of the unfolded protein.

Consequently, least-squares analysis must be conducted on truncated heat capacity files. The previous analysis of Phl p 7 returned a low value for the ΔC_p, 0.20 kcal mol^{-1} K^{-1}. Although this result was qualitatively consistent with the enhanced thermal stability of the stability, we were concerned that the absence of posttransition baseline data compromised our estimate of ΔC_p.

To improve our parameter estimates, we supplemented the DSC data with urea denaturation data. The application of chemical denaturation data to the determination of ΔC_p was originally suggested by Pace and Laurents (*27*). The strategy that we employed is modeled after the analysis by McCrary et al. (*28*). Samples were titrated with urea, and the resulting ellipticity data were analyzed simultaneously with the DSC data. The following equation for a two-state unfolding transition (*29*) was used to treat the chemical denaturation data:

$$y = \frac{(y_n + m_n[\text{urea}]) + (y_u + m_u[\text{urea}])\exp(-(\Delta G_o - m[\text{urea}])/RT)}{1 + \exp(-(\Delta G_o - m[\text{urea}])/RT)} \quad (3)$$

where ΔG_o is the conformational stability in the absence of urea, m is the sensitivity of the protein to the denaturant concentration, y_n and m_n are the intercept and slope of the pretransition baseline, and y_u and m_u are the corresponding values for the posttransition baseline. Instead of treating ΔG_o as a fitting parameter, its value was calculated using the Gibbs−Helmholtz equation:

$$\Delta G_o = \Delta H_{vH}\left(1 - \frac{T}{T_m}\right) + \Delta C_p[(T - T_m) - T\ln(T/T_m)] \quad (4)$$

Thus, least-squares minimization selects for values of T_m, ΔH_{vH}, and ΔC_p that are consistent with both the chemical and thermal denaturation data. Phl p 7 and Phl p 7 D55S were each titrated with urea at 40, 45, 50, 55, and 60 °C. The other three proteins, for which posttransition baseline data were available, were titrated with urea at a single temperature (25 °C). Parameter uncertainties were evaluated by confidence interval analysis, as described above.

To examine the impact of Ca^{2+} on stability by DSC, the proteins were first dialyzed extensively against HBS containing 0.005 M EDTA and then against three changes of HBS containing 20 μM Ca^{2+}.

RESULTS

Sedimentation Equilibrium Analyses. Samples of Bet v 4, Bra n 1, and Bra n 2 and the D55S variant of Phl p 7 were sedimented to equilibrium in the presence and absence of Ca^{2+}. In every case, the data were satisfactorily accommodated by an ideal single species model, yielding an average molecular weight consistent with a monomeric quaternary structure. Radial solute distributions for the Ca^{2+}-bound proteins are displayed in Figure 2. Bet v 4, with a sequence-derived molecular mass of 9316 Da, exhibited apparent molecular weights of 9250 ± 60 and 9330 ± 70 in the Ca^{2+}-free and -bound states, respectively. Bet v 4 has been examined previously by analytical ultracentrifugation (*30*). Our results are entirely consistent with the earlier study. The analyses of Bra n 1 yielded corresponding values of 8590 ± 30 and 8610 ± 30; Bra n 2 afforded values of 9090 ± 70 and 9240 ± 70, and Phl p 7 D55S afforded values of 8520 ± 30 and 8610 ± 40.

Divalent Ion Binding. The divalent ion-binding properties of Bet v 4, Bra n 1, Bra n 2, and the D55S variant of Phl p 7 were characterized by isothermal titration calorimetry. Raw data from

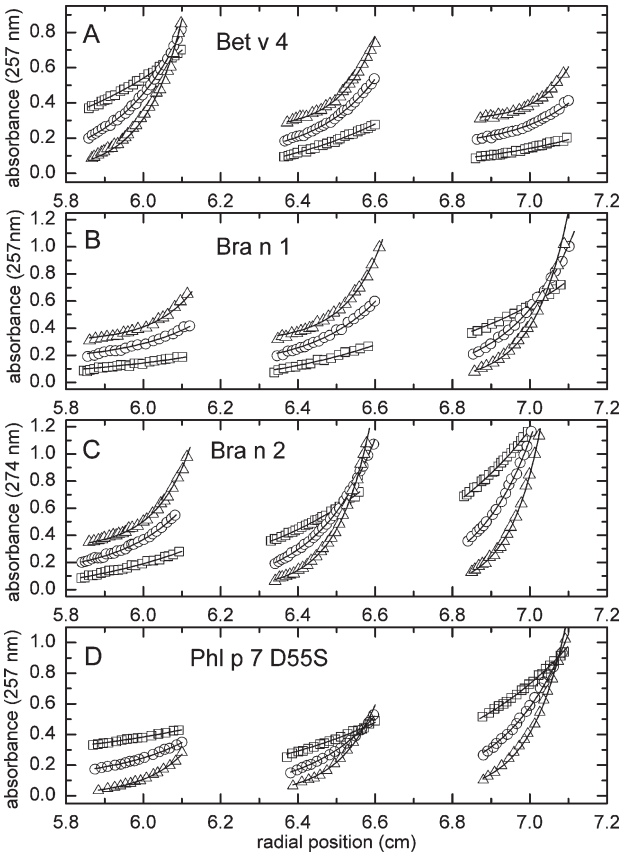

FIGURE 2: Sedimentation equilibrium analyses of Bet v 4 (A), Bra n 1 (B), Bra n 2 (C), and Phl p 7 D55S (D). Samples of the proteins were sedimented to equilibrium, at 20 °C, at rotor speeds of 20000 (□), 30000 (○), and 40000 (△) rpm, in Hepes-buffered saline, pH 7.4, containing 100 μM Ca^{2+}. In some cases, the data and least-squares fits have been offset vertically for clarity.

the titrations of each protein with Ca^{2+} and Mg^{2+} are displayed in Figure 3. For comparison, corresponding data for Phl p 7 have also been included. The proteins exhibit pronounced differences in Ca^{2+}-binding enthalpy. Notably, the enthalpy associated with the second Ca^{2+}-binding event in both Bet v 4 and Bra n 2 is substantially more exothermic than that associated with the initial binding event. By contrast, the binding enthalpies in Bra n 1 and Phl p 7, wild type and D55S, are more comparable in magnitude.

Binding parameters were estimated for each protein by global least-squares minimization of ITC data. A representative analysis, for Bra n 2, is displayed in Figure 4. The resulting parameters and parameter uncertainties for all of the proteins, including Phl p 7, are listed in Table 1. Divalent ion-binding energetics for Bet v 4, Bra n 1, Bra n 2, Phl p 7, and Phl p 7 D55S are summarized in Figure 5. Corresponding numerical values are presented in Table 2.

As explained in Materials and Methods, during the least-squares analyses conducted as part of this study, we allowed the enthalpy change associated with the formation of the mixed Ca^{2+}−Mg^{2+} species to float. In our previous analysis of Phl p 7, we had set this value at the sum of the enthalpy changes for first Ca^{2+}-binding event and the second Mg^{2+}-binding event. Upon reflection, it eventually occurred to us that there was, in fact, no cogent basis for that simplification of the data treatment. Mixed species can, in principle, be formed during the titrations with Ca^{2+} conducted in the presence of fixed levels of Mg^{2+}. The exact nature of the species, i.e., whether sites 1 and 2 are occupied by

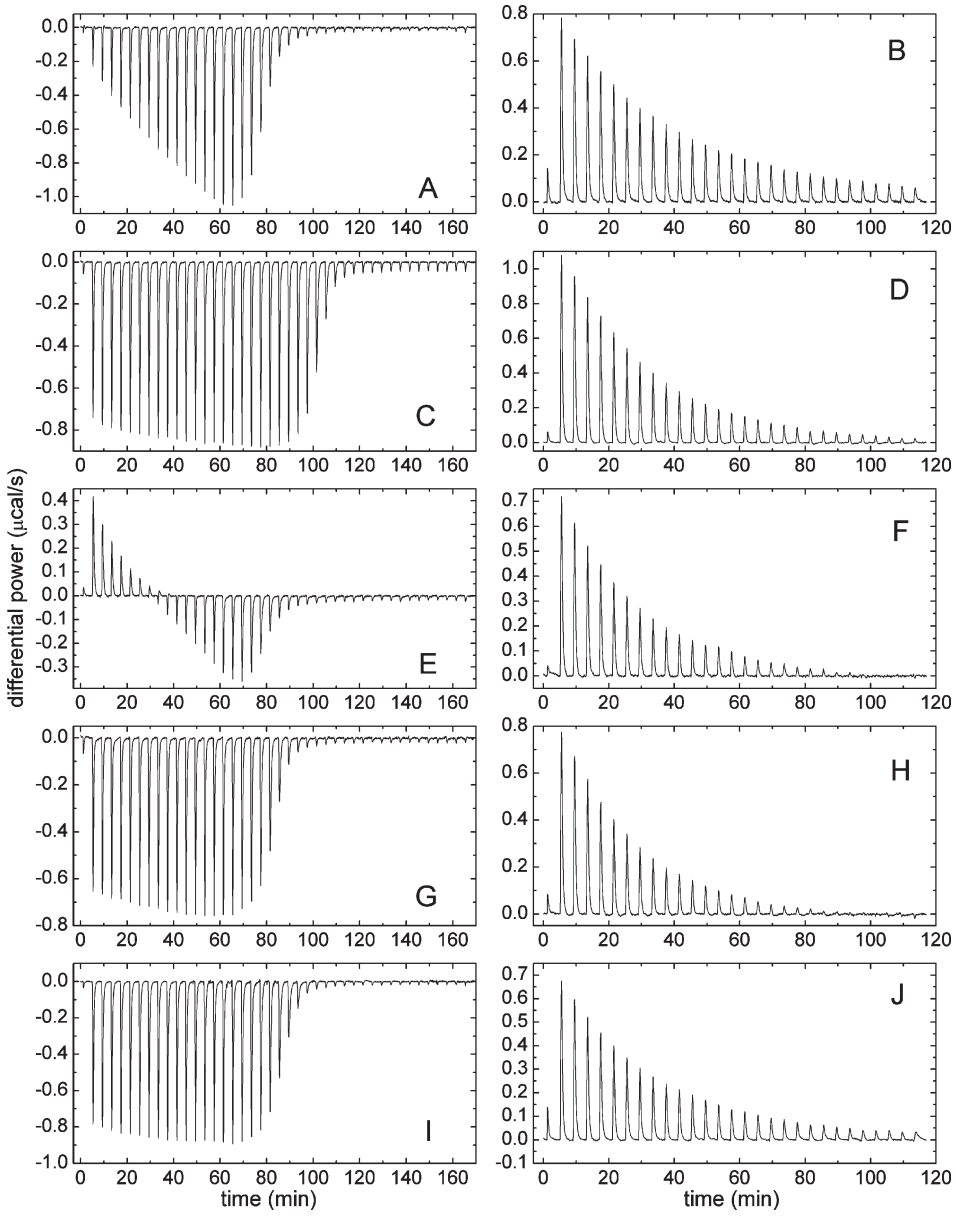

FIGURE 3: Raw ITC data. Titration of Bet v 4 with Ca^{2+} (A) and Mg^{2+} (B); titration of Bra n 1 with Ca^{2+} (C) and Mg^{2+} (D); titration of Bra n 2 with Ca^{2+} (E) and Mg^{2+} (F); titration of Phl p 7 with Ca^{2+} (G) and Mg^{2+} (H); titration of Phl p 7 D55S with Ca^{2+} (I) and Mg^{2+} (J).

Ca^{2+} or Mg^{2+}, is not readily predictable and could vary during the course of the titration.

Allowing the heat associated with formation of the mixed species to float significantly lowered the reduced chi square value for the Phl p 7 analysis. Unsurprisingly, the improvement was reflected primarily in the quality of the fit to the Ca^{2+}-binding data collected in the presence of Mg^{2+}. Inclusion of the additional fitting parameter had a perceptible impact on the resulting estimates for the binding constants. The Ca^{2+}-binding constants changed from 1.73×10^6 and 8.06×10^6 M^{-1} to 1.90×10^6 and 6.44×10^6 M^{-1}. The influence on the Mg^{2+}-binding parameters was larger, moving from 2.77×10^4 and 170 M^{-1} to 1.25×10^4 and 131 M^{-1}. The average formation constant for the mixed Ca^{2+}–Mg^{2+} species, previously 1.08×10^9 M^{-2}, increased to 4.53×10^9 M^{-2}.

Tables 1 and 2 are noteworthy for the absence of large differences in divalent ion-binding behavior among the four polcalcin isoforms. The overall standard free energies for Ca^{2+} binding span the narrow range between −17.3 and −18.2 kcal/mol. The overall Mg^{2+} affinities are likewise tightly clustered, ranging from −8.1 to −8.6 kcal/mol. These data suggest that the divalent ion-binding signature of Phl p 7 is quite unremarkable. In light of the major impact resulting from introduction of a fifth anionic ligand into the parvalbumin metal ion-binding sites, this finding was unexpected.

To better assess the impact of the additional carboxylate side chain in site 2 of Phl p 7, we characterized the D55S variant, in which the aspartyl residue at the $-x$ position has been replaced by the consensus residue, serine. Whereas elimination of the anionic residue would lower Ca^{2+} affinity in the parvalbumin background, it actually improves the overall standard free energy for Ca^{2+} binding from −17.84 (±0.13) to −18.17 (±0.13) kcal/mol in the context of Phl p 7. Overall Mg^{2+} affinity, which is highly sensitive to the presence or absence of the additional carboxylate in the parvalbumin CD site, is unaltered by the substitution.

If the two polcalcin EF-hands had the same intrinsic affinity for Ca^{2+}, then the macroscopic association constants should differ by a factor of 4; i.e., K_2 would equal $0.25K_1$. Thus, if K_2 is

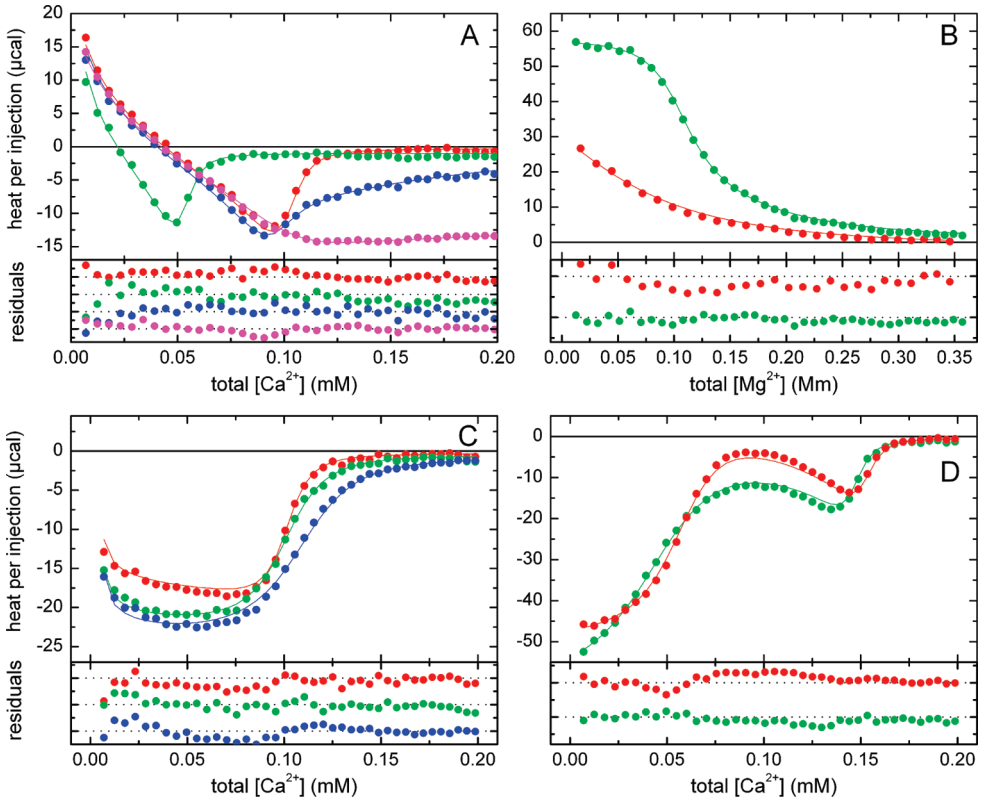

FIGURE 4: Analysis of divalent ion binding by Bra n 2. (A) Titration with 1.10 mM Ca^{2+}: 56 μM Bra n 2 (red); 27 μM Bra n 2 (green); 55 μM Bra n 2, 0.10 mM NTA (blue); 55 μM Bra n 2, 1.0 mM NTA (pink). (B) Titration with 1.99 mM Mg^{2+}: 56 μM Bra n 2 (red); 55 μM Bra n 2, 100 μM EDTA (green). (C) Titration with 1.10 mM Ca^{2+} in the presence of Mg^{2+}: 54 μM Bra n 2, 1.00 mM Mg^{2+} (red); 53 μM Bra n 2, 5.00 mM Mg^{2+} (green); 55 μM Bra n 2, 10.0 mM Mg^{2+} (blue). (D) Titration with 1.10 mM Ca^{2+}: 55 μM Bra n 2, 60 μM EDTA (red); 60 μM Bra n 2, 60 μM EGTA (green).

Table 1: Divalent Ion-Binding Properties

protein	K_1[a] (M^{-1})	ΔH_1 (kcal/mol)	K_2[a] (M^{-1})	ΔH_2 (kcal/mol)	K_{1M}[a] (M^{-1})	ΔH_{1M} (kcal/mol)	K_{2M}[a] (M^{-1})	ΔH_{2M} (kcal/mol)	β_{CM} (M^{-1})	ΔH_{CM} (kcal/mol)
Bet v 4	5.13×10^6	0.42	2.68×10^6	−6.28	8.50×10^3	4.78	106	3.58	8.50×10^8	6.52
	(4.77, 5.49)	(0.35, 0.49)	(2.44, 2.95)	(−6.41, −6.16)	(7.82, 9.18)	(4.64, 4.93)	(87, 122)	(3.22, 3.93)	(6.97, 10.0)	(5.34, 7.43)
Bra n 1	2.65×10^6	−2.37	7.76×10^6	−4.30	1.75×10^4	3.90	98	6.65	4.03×10^9	6.50
	(2.45, 2.78)	(−2.44, −2.27)	(7.29, 8.45)	(−4.40, −4.21)	(1.66, 1.87)	(3.82, 3.99)	(92, 106)	(6.25, 6.91)	(3.83, 4.35)	(6.09, 6.76)
Bra n 2	2.40×10^6	2.63	2.04×10^6	−3.28	1.16×10^4	3.80	190	3.05	9.00×10^8	4.82
	(2.26, 2.55)	(2.55, 2.72)	(1.84, 2.27)	(−3.38, −3.19)	(1.06, 1.26)	(3.68, 3.92)	(157, 220)	(2.84, 3.29)	(7.02, 12.5)	(4.39, 5.79)
Phl p 7	1.90×10^6	−1.96	6.44×10^6	−3.95	1.76×10^4	3.24	84	6.63	4.53×10^9	0.59
	(1.71, 2.09)	(−2.07, −1.85)	(5.72, 7.27)	(−4.07, −3.84)	(1.58, 1.92)	(3.14, 3.34)	(76, 92)	(6.24, 7.08)	(3.72, 5.71)	(0.34, 0.83)
Phl p 7 D55S	3.44×10^6	−2.73	6.17×10^6	−4.47	1.25×10^4	3.23	131	3.98	4.98×10^9	0.35
	(3.19, 3.82)	(−2.83, −2.62)	(5.68, 6.98)	(−4.57, −4.36)	(1.16, 1.37)	(3.13, 3.36)	(119, 147)	(3.67, 4.24)	(4.23, 5.82)	(0.11, 0.53)

[a]Stepwise macroscopic association constants.

greater than $0.25K_1$, the system exhibits macroscopic positive cooperativity, and the apparent coupling free energy is equal to $-RT \ln(4K_2/K_1)$. This value reflects the minimum coupling free energy because it is likely that the two sites have intrinsically different Ca^{2+} affinity.

Inspection of Table 1 reveals that all four polcalcin isoforms exhibit macroscopically cooperative Ca^{2+} binding. However, the magnitudes of the apparent coupling free energies measured for Bet v 4 (-0.44 ± 0.10 kcal/mol) and Bra n 2 (-0.72 ± 0.10 kcal/mol) are significantly smaller than those of Bra n 1 (-1.46 ± 0.09 kcal/mol) and Phl p 7 (-1.54 ± 0.14 kcal/mol). The D55S mutation reduces the magnitude of the coupling free energy in Phl p 7 to -1.17 ± 0.11 kcal/mol.

Impact of Phl p 7 D55S, Bet v 4, Bra n 1, and Bra n 2 on ANS Emission. As observed previously for Phl p 7, addition of the Ca^{2+}-bound proteins to samples of ANS provokes a significant increase in fluorescence emission. Whereas Bet v 4 and Bra n 1 had comparable effects on ANS quantum yield, Bra n 2 produced a substantially larger increase. The intensity of the emission spectrum observed in the presence of Bra n 2 (Figure 6A) was approximately 3-fold higher than those observed in the presence of either Bet v 4 or Bra n 1. Additionally, the peak maximum was shifted to perceptibly shorter wavelength.

Conformational Stability. The stabilities of Bet v 4, Bra n 1, and Bra n 2 were examined by DSC. Each protein was analyzed at four protein concentrations (Figure 7, panels A−C) in PBS containing 5.0 mM EDTA. The resulting data were subjected to global least-squares minimization to obtain estimates for the melting temperature (T_m), the van't Hoff enthalpy (ΔH_{vH}), the calorimetric enthalpy (ΔH_{cal}), and the denaturational heat

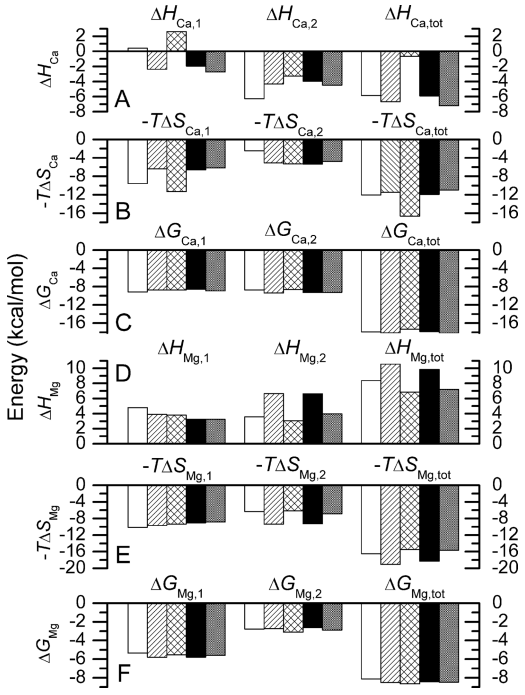

FIGURE 5: Comparison of divalent ion-binding energetics for Bet v 4 (white), Bra n 1 (diagonal shading), Bra n 2 (cross-hatch), Phl p 7 (black), and Phl p 7 D55S (dark gray).

capacity increment (ΔC_p), which are listed in Table 3. The resulting values were then substituted into eq 3 to calculate the conformational stabilities for the Ca^{2+}-free proteins at 25 °C. The thermal stability parameters are plotted in Figure 8.

The stability of Phl p 7 was also re-examined, employing simultaneous least-squares analysis of DSC and chemical denaturation data, with the goal of obtaining a more reliable estimate of ΔC_p. That analysis, the details of which are described in Materials and Methods, is displayed in Figure 7E and 7G. Inclusion of the urea denaturation data, intended to compensate for the dearth of posttransition baseline data, has a significant impact on the fitting parameters. The composite analysis affords a T_m of 77.3 ± 0.3 °C, as compared to the value of 78.5 °C reported previously. The estimate for the van't Hoff enthalpy, at 52.1 ± 1.3 kcal/mol, is somewhat lower than the previously determined value of 55.6 kcal/mol. By contrast, the calorimetric enthalpy, at 61.3 ± 0.8 kcal/mol, is substantially higher than the previous estimate of 54.5 kcal/mol. The value obtained for ΔC_p (0.34 ± 0.03 kcal mol^{-1} K^{-1}) is substantially lower than the values obtained for the other three polcalcin isoforms but somewhat higher than the estimate obtained by analysis of the DSC data alone (0.20 kcal mol^{-1} K^{-1}).

The stability of Phl p 7 D55S was also evaluated by global analysis of DSC and urea denaturation data (Figure 7F,H). Replacement of Asp-55 by serine has a minor impact on Phl p 7 stability. The T_m increases by 0.7 degree, to 78.0 ± 0.2 °C. ΔH_{vH} is increased to 54.6 ± 0.3 kcal/mol, whereas ΔH_{cal} decreases to 56.1 ± 1.1 kcal/mol. The value obtained for ΔC_p (0.32 ± 0.08 kcal mol^{-1} K^{-1}) remains low by comparison to the other three polcalcins.

The ratio of the van't Hoff and calorimetric enthalpies furnishes information on the size of the cooperative unit involved in unfolding. Values close to unity indicate that denaturation is two state, proceeding directly from the native to the unfolded state. Ratios less than one imply that the unfolding occurs with significant population of partially unfolded intermediates. Values greater than one, on the other hand, imply that denaturation proceeds from an oligomeric state to the unfolded state. The $\Delta H_{vH}/\Delta H_{cal}$ ratios obtained for Bet v 4, Bra n 1, Bra n 2, and the D55S variant of Phl p 7 range between 0.97 ± 0.02 and 1.00 ± 0.04, indicating that thermal denaturation of these Ca^{2+}-free polcalcins closely approximates a two-state process. The ratio obtained for Phl p 7 is somewhat lower (0.85 ± 0.06), suggesting that unfolding of the protein is accompanied by higher population of partially unfolded intermediates.

Table 2: Divalent Ion-Binding Energetics[a]

	Ca^{2+} binding			Mg^{2+} binding		
protein	ΔG^b	ΔH	$-T\Delta S^c$	$\Delta G^{o\prime}$	ΔH	$-T\Delta S$
Binding Event 1						
Bet v 4	−9.15 (0.04)	0.42	−9.57	−5.36 (0.05)	4.78	−10.14
Bra n 1	−8.76 (0.05)	−2.37	−6.39	−5.79 (0.04)	3.90	−9.69
Bra n 2	−8.70 (0.04)	2.63	−11.33	−5.54 (0.05)	3.80	−9.34
Phl p 7	−8.56 (0.06)	−1.96	−6.60	−5.79 (0.06)	3.24	−9.03
Phl p 7 D55S	−8.91 (0.06)	−2.73	−6.18	−5.59 (0.05)	3.23	−8.82
Binding Event 2						
Bet v 4	−8.76 (0.06)	−6.28	−2.48	−2.76 (0.12)	3.58	−6.34
Bra n 1	−9.39 (0.05)	−4.30	−5.09	−2.71 (0.05)	6.65	−9.36
Bra n 2	−8.60 (0.06)	−3.28	−5.32	−3.11 (0.11)	3.05	−6.16
Phl p 7	−9.28 (0.07)	−3.95	−5.33	−2.62 (0.06)	6.63	−9.25
Phl p 7 D55S	−9.26 (0.07)	−4.47	−4.79	−2.89 (0.07)	3.98	−6.87
Overall						
Bet v 4	−17.91 (0.10)	−5.86	−12.05	−8.12 (0.17)	8.36	−16.48
Bra n 1	−18.15 (0.10)	−6.67	−11.48	−8.50 (0.09)	10.55	−19.05
Bra n 2	−17.30 (0.10)	−0.65	−16.65	−8.65 (0.16)	6.85	−15.50
Phl p 7	−17.84 (0.13)	−5.91	−11.93	−8.41 (0.12)	9.87	−18.28
Phl p 7 D55S	−18.17 (0.13)	−7.20	−10.97	−8.47 (0.12)	7.21	−15.68

[a]Energies in kcal/mol. Binding data were collected in Hepes-buffered saline, pH 7.4, at 25 °C. [b]Equal to $-RT\ln K$, where R is the gas constant, T the absolute temperature, and K the relevant macroscopic binding constant. Uncertainties are shown in parentheses. [c]Equal to $\Delta G - \Delta H$.

Samples of the proteins were also examined in the presence of 20 μM Ca^{2+} (Figure 7D). The observed T_m values range from 106° for Bra n 2 to 107° for Bet v 4 to 116° for Bra n 1. The D55S mutation evidently increases the T_m of Ca^{2+}-bound Phl p 7. Whereas the heat capacity curve for the wild-type Phl p 7 solution is approaching its maximum at 120 °C, the high-temperature limit for our calorimeter, the heat capacity of the Phl p 7 D55S sample is still increasing, with no clear indication of an inflection point.

DISCUSSION

The consensus residue at the $-x$ coordination position in polcalcin EF-hand 2 is serine. In Phl p 7, however, aspartate occupies the $-x$ position. Consequently, the site 2 ion-binding loop in Phl p 7 harbors five potential anionic ligands, rather than four. In fact, the crystal structure of Ca^{2+}-bound Phl p 7 (*31*) reveals that just four of the five participate directly in metal ion binding. The $-x$ carboxylate has withdrawn from the coordination sphere and functions as a helix cap, hydrogen bonding to the amide proton of the $-z$ glutamyl residue. Similar coordination geometry is observed for the CD site of rat α-PV S55D/E59D (*32*), which likewise includes five anionic residues.

The pentacarboxylate site confers heightened divalent ion affinity on the rat α- and β-parvalbumin isoforms. To determine

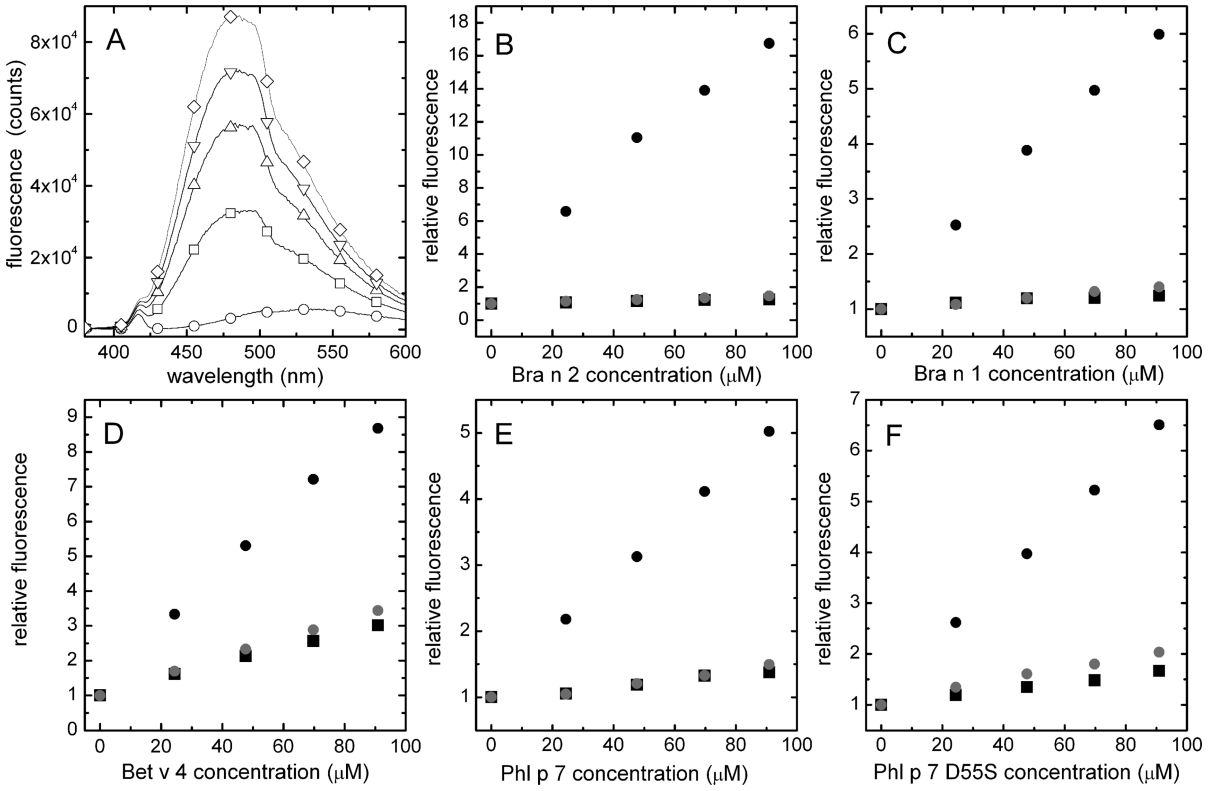

FIGURE 6: Impact of polcalcin on ANS emission. (A) Ca^{2+}-free Bra n 2 was added to 10 μM ANS (○) in Hepes-buffered saline, pH 7.4, 200 μM Ca^{2+}, to yield nominal final concentrations of 25 (□), 50 (△), 75 (▽), and 100 (◇) μM. The emission spectrum was acquired following each addition, exciting at 365 nm. (B) Relative intensity at the emission maximum vs Bra n 2 concentration in 200 μM Ca^{2+} (black circle), 50.0 mM EDTA (black square), and 1.0 M EGTA, 2.0 mM Mg^{2+} (gray circle). Comparable studies were also conducted with Bra n 1 (C), Bet v 4 (D), Phl p 7 (E), and Phl p 7 D55S (F).

whether the introduction of the additional carboxylate has a similar impact in the polcalcin background, we have compared the metal ion-binding signatures of Phl p 7 and three additional isoforms. Although the aligned polcalcin core sequences exhibit roughly 70% identity, they harbor short N-terminal extensions of varying length. Relative to Phl p 7, perhaps the shortest member of the polcalcin family, the sequences of Bra n 1, Bra n 2, and Bet v 4 contain one, five, and seven additional residues, respectively, at the N-terminal end (Figure 1A).

The four polcalcins exhibit similar divalent ion-binding behavior. The standard free energy change for Ca^{2+} binding ranges between -17.3 ± 0.1 and -18.2 ± 0.1 kcal mol^{-1}; the corresponding Mg^{2+} value ranges from -8.1 ± 0.2 to -8.6 ± 0.2 kcal mol^{-1}. The divalent ion-binding properties of Phl p 7 are unexceptional. At -17.8 ± 0.1 kcal mol^{-1}, overall Ca^{2+} affinity is exceeded by both Bet v 4 and Bra n 1; overall Mg^{2+} affinity, at -8.4 ± 0.1 kcal mol^{-1}, is exceeded both by Bra n 1 and Bra n 2. Evidently, substitution of aspartate for the consensus serine at the $-x$ position in Phl p 7 site 2 does not produce a protein with anomalously high divalent ion affinity.

To obtain further insight into this issue, we examined the impact of replacing D55 in Phl p 7 with serine. Based upon the behavior of the pentacarboxylate PV variants, removal of the fifth carboxylate in Phl p 7 site 2 was predicted to cause a significant reduction in divalent ion affinity. Unexpectedly, the D55S mutation affords a perceptible increase in Ca^{2+} affinity, from -17.8 to -18.2 ± 0.1 kcal mol^{-1}, and leaves the Mg^{2+} affinity essentially unchanged. In fact, the binding properties of Phl p 7 D55S strongly resemble those of Bra n 1.

The D55S substitution in Phl p 7 is analogous to reversal of the G98D variant in the parvalbumin molecule. In rat β-PV, for example, that reversal decreases Ca^{2+} affinity by 1.3 kcal mol^{-1}. As illustrated in Figure 9A, the reduction in affinity derives from a 0.4 kcal mol^{-1} stabilization of the unliganded protein, presumably by diminished electrostatic repulsion, and 0.9 kcal mol^{-1} stabilizing of the bound protein, presumably by the aforementioned hydrogen bonding between the $-x$ carboxylate and the amide proton of the $-z$ glutamate.

Correspondingly, one anticipates that replacement of D55 by serine in Phl p 7 would stabilize the protein by reducing electrostatic repulsion in site 2. Consistent with that expectation, the extrapolated stability for the apo-D55S variant is 0.5 kcal/mol greater than that of wild-type Phl p 7 at 25 °C. The side-chain entropies of serine and aspartate are comparable, and the ΔC_p for unfolding is virtually unchanged by the mutation, implying that the increased stability of apo-D55S reflects stabilization of the folded apoprotein. As shown in Figure 9B, this stabilization of the Ca^{2+}-free protein, coupled with the 0.4 kcal mol^{-1} increase in Ca^{2+} affinity, positions the free energy of the Ca^{2+}-bound D55S variant approximately 1.0 kcal mol^{-1} lower than the wild-type protein.

Thus, replacement of the $-x$ aspartyl residue has a disparate impact on the bound form of the protein depending on whether it is performed in the polcalcin or parvalbumin background. Whereas the modification destabilizes the Ca^{2+}-bound form of rat β-PV G98D by 0.9 kcal/mol, it increases the stability of Ca^{2+}-bound Phl p 7 by roughly that same amount. Parenthetically, the heightened stability of the Ca^{2+}-bound variant is consistent with the limited DSC data available for the Ca^{2+}-bound proteins. As shown in Figure 7D, the T_m for Phl p 7 D55S occurs at higher temperature than that observed with the wild-type protein in the presence of Ca^{2+}.

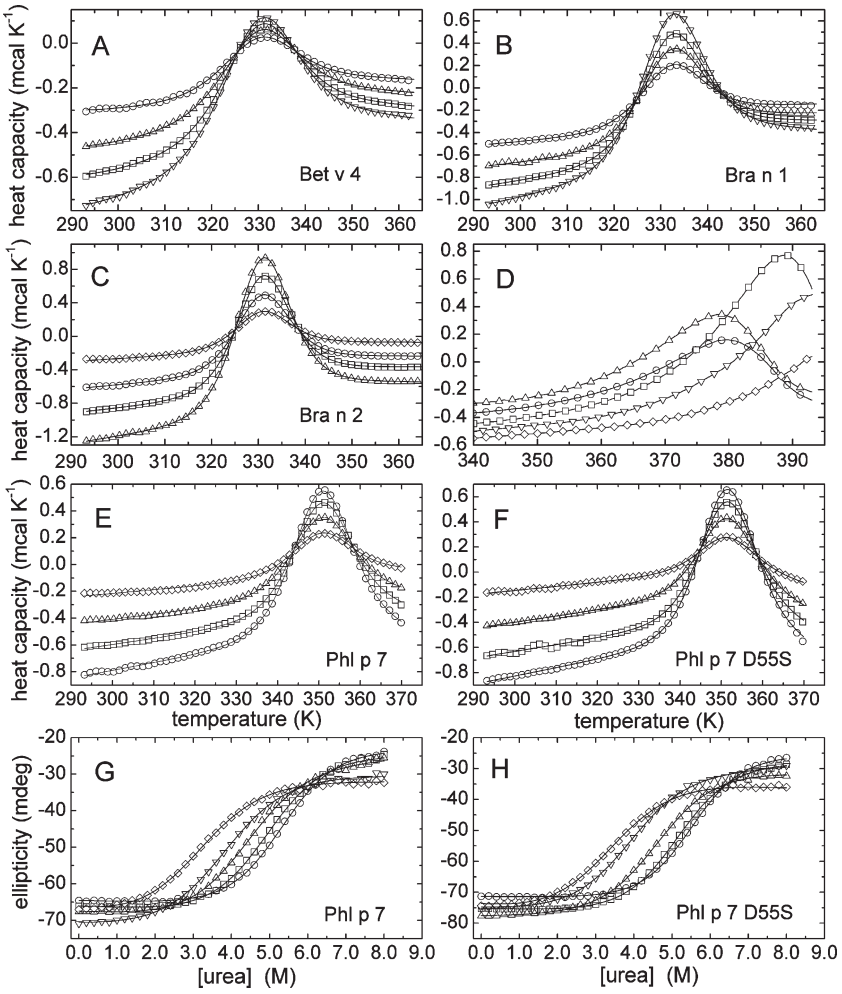

FIGURE 7: Polcalcin conformational stability. (A) DSC analysis of Bet v 4 in PBS/EDTA, pH 7.4, at 6.98 mg/mL (▽), 5.59 mg/mL (□), 4.19 mg/mL (△), and 2.79 mg/mL (○). (B) DSC analysis of Bra n 1 under identical solution conditions at 9.17 mg/mL (▽), 6.88 mg/mL (□), 4.95 mg/mL (△), and 2.47 mg/mL (○). (C) DSC analysis of Bra n 2 in PBS/EDTA at 12.4 mg/mL (△), 9.3 mg/mL (□), 6.2 mg/mL (○), and 3.1 mg/mL (◇). (D) DSC analysis of Ca^{2+}-bound polcalcins. Each protein was dialyzed to equilibrium against HBS, pH 7.4, containing 20 μM Ca^{2+}. Bet v 4 (5.76 mg/mL, ○); Bra n 1 (6.56 mg/mL, □); Bra n 2 (6.17 mg/mL, △); Phl p 7 (4.30 mg/mL, ▽); Phl p 7 D55S (4.97 mg/mL, ◇). Solid lines have been included solely to guide the eye. (E) DSC analysis of Phl p 7 in PBS/EDTA, pH 7.4, at 7.86 mg/mL (○), 5.89 mg/mL (□), 3.89 mg/mL (△), and 1.96 mg/mL (◇). (F) DSC analysis of Phl p 7 D55S in PBS/EDTA at 9.1 mg/mL (○), 6.82 mg/mL (□), 4.55 mg/mL (△), and 2.27 mg/mL (◇). (G) Urea denaturation of Phl p 7 in PBS/EDTA at 40 (○), 45 (□), 50 (△), and 55 (▽), and 60 °C (◇). (H) Urea denaturation of Phl p 7 D55S in PBS/EDTA at 40 (○), 45 (□), 50 (△), and 55 (▽), and 60 °C (◇). The DSC data in panels E and F were simultaneously fit along with the urea denaturation data in panels G and H, respectively, as described in the text. Similarly, the DSC data in panels A−C were simultaneously fit with urea denaturation data (not shown) collected at 25 °C. For clarity, a small subset of the data is displayed in panels A−C, E, and F. Similarly, every other data point is included in panels G and H.

Table 3: Summary of Polcalcin DSC Analyses[a]

protein	T_m	ΔH_{vH}	ΔH_c	$\Delta H_{vh}/\Delta H_c$	ΔC_p	ΔG_{conf}[b]
Bet v 4	56.1	43.9	43.7	1.00	0.66	3.1 ± 0.2
	(55.9, 56.4)	(43.2, 44.2)	(42.6, 45.3)	(0.95, 1.04)	(0.55, 0.74)	
Bra n 1	57.9	48.7	49.9	0.98	0.95	3.2 ± 0.2
	(57.7, 58.9)	(48.3, 49.2)	(48.6, 51.3)	(0.94, 1.01)	(0.87, 1.00)	
Bra n 2	56.8	56.1	55.9	1.00	0.95	3.9 ± 0.2
	(56.6, 57.1)	(55.3, 56.9)	(54.6, 57.2)	(0.97, 1.04)	(0.88, 1.01)	
Phl p 7	77.3	52.1	61.3	0.85	0.34	6.4 ± 0.3
	(77.0, 77.6)	(51.0, 52.4)	(60.7, 64.2)	(0.79, 0.86)	(0.31, 0.37)	
Phl p 7 D55S	78.0	54.6	56.1	0.97	0.32	6.9 ± 0.4
	(77.8, 78.2)	(54.3, 54.9)	(55.6, 57.2)	(0.95, 0.98)	(0.26, 0.40)	

[a]Temperatures are reported in °C, energies in kcal mol^{-1}, and ΔC_p in kcal mol^{-1} K^{-1}. The 95% confidence intervals are shown in parentheses. [b]Apparent conformational stability at 25 °C, calculated with eq 4.

The differing impact of the removal of the $-x$ carboxylate in the parvalbumin and polcalcin backgrounds may reflect the allosteric nature of polcalcin Ca^{2+} binding; i.e., the first Ca^{2+}-binding event is linked to a major conformational change that facilitates the second binding event. Indeed, the fact that Mg^{2+} affinity is unchanged by the D55S mutation suggests that the

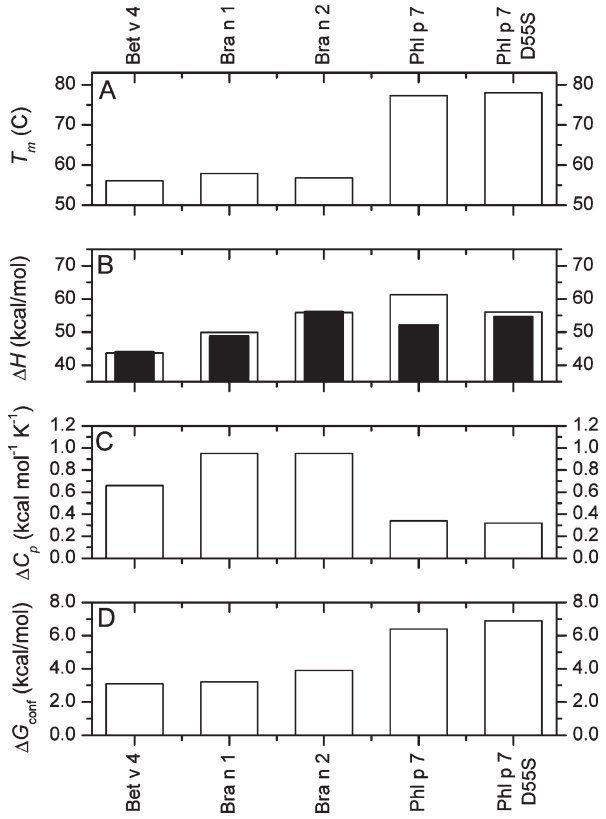

FIGURE 8: Summary of polcalcin thermal stability analysis. (A) Melting point. (B) Denaturational enthalpies: van't Hoff (black); calorimetric (white). (C) Denaturational heat capacity increment. (D) Extrapolated conformational stability at 25 °C, calculated with eq 3.

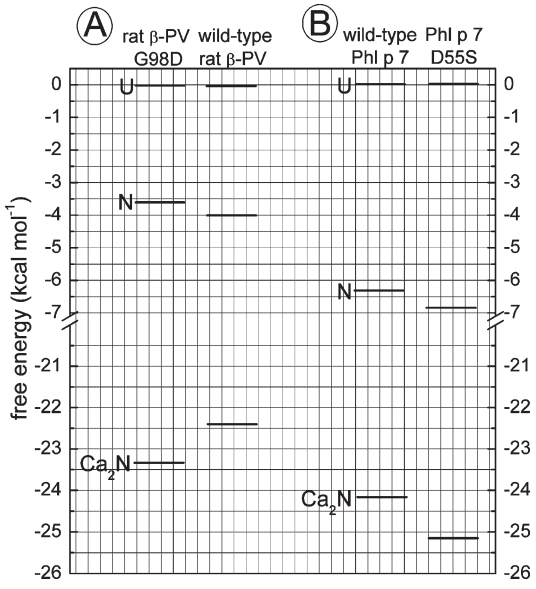

FIGURE 9: Free energy diagrams comparing the relative energies of the unfolded state (U), the unliganded native state (N), and the Ca^{2+}-loaded state (Ca_2N). The analysis neglects the impact of replacement of the $-x$ aspartyl residue on the denatured ensemble. (A) The G98D variant of rat β-PV and wild-type rat β-PV. (B) Wild-type Phl p 7 and the D55S variant of Phl p 7.

energetic difference is related to the Ca^{2+}-triggered conformational change. We have previously noted that Mg^{2+} binding does not provoke a similar structural modification in Phl p 7 (*14*).

As discussed previously (*14*), the major unliganded polcalcin conformation evidently has low affinity for Ca^{2+}, requiring the sacrifice of binding free energy to promote a transition to a conformation competent for Ca^{2+} binding. Data for model EF-hand peptide systems indicate that EF-hand binding loops containing four coordinating carboxylates possess greater affinity for Ca^{2+} results than sites containing just three (*33*−*35*). Thus, it is likely that polcalcin site 2 is preferentially occupied by Ca^{2+}, at least in Bet v 4, Bra n 2, and Phl p 7. Both sites in Bra n 1 harbor four coordinating carboxylates. *A priori*, an increase in the Ca^{2+} affinity of site 2, by introduction of an additional carboxylate to the coordination sphere, should increase the affinity of the first binding event. In fact, the free energy change associated with the initial Ca^{2+}-binding event is lower for Phl p 7 than that measured for the other three polcalcin isoforms. In this context, it is noteworthy that the heightened Ca^{2+} affinity of the D55S variant is realized in the first binding event. The second binding event is isoenergetic for the wild-type and variant proteins.

It is possible that formation of the H-bond between the carboxylate of D55 and the amide of E58 requires an additional conformational adjustment not required for polcalcin isoforms harboring the consensus serine residue at $-x$ in site 2. High-resolution structural data for Ca^{2+}-free and Ca^{2+}-bound Phl p 7 might provide some insight into this question.

At present, there are no structural data for the unliganded protein, and under the conditions employed for crystallization of the Ca^{2+}-bound protein, Phl p 7 partially unfolds and assumes an unusual domain-swapped dimeric structure (*31*). The characteristic intramolecular pairing of the two EF-hand motifs has been lost, replaced by a pairing of site 1 from one monomer and site 2 from the other. Because sedimentation equilibrium data for Phl p 7 clearly indicate that Phl p 7 is monomeric in saline at neutral pH, the physiological significance of the domain-swapped dimer is questionable. Although, as noted above, the hydrogen bond between the carboxylate of D55 and the amide proton of E58 is observed in the crystal structure of the Ca^{2+}-bound state, it may not be formed in the monomeric Ca^{2+}-bound protein. Clearly, additional structural data are needed for the Ca^{2+}-bound Phl p 7 monomer.

A secondary objective of this study was to explore the influence, if any, of the N-terminal extension on polcalcin divalent ion-binding behavior. Although there is no correlation between overall divalent ion affinity, either for Ca^{2+} or Mg^{2+}, and the length of the N-terminal extension, the second Ca^{2+}-binding event is 0.5−0.8 kcal mol^{-1} less favorable for the two proteins with the longer extension, Bet v 4 and Bra n 2. This difference is likewise reflected in the magnitudes of the minimal coupling free energies, which are significantly smaller for Bet v 4 and Bra n 2 (-0.44 ± 0.10 and -0.72 ± 0.10 kcal mol^{-1}, respectively) than those of Bra n 1 and Phl p 7 (-1.46 ± 0.09 and -1.54 ± 0.14 kcal mol^{-1}, respectively). Relative to the other two proteins, the conformational change associated with the initial Ca^{2+}-binding event in either Bet v 4 or Bra n 2 evidently does not produce a conformation as well suited for binding of the second Ca^{2+}.

The Ca^{2+}-binding enthalpies are interesting. Whereas the initial binding event is exothermic for the two shorter polcalcins, it is endothermic for Bet v 4 and Bra n 2. In fact, the initial binding enthalpy for Bra n 2 is sufficiently endothermic (2.6 ± 0.1 kcal/mol) that the overall binding enthalpy is just slightly exothermic (-0.6 ± 0.1 kcal/mol). Interestingly, however, the endothermic ΔH terms do not impose a free energy penalty, as they are balanced by a proportionally more favorable entropy

change. Consequently, the resulting free energy changes ($\Delta G_{Ca,1}$) associated with Bet v 4 and Bra n 2 are comparable to those observed for Bra n 1 and Phl p 7, and $\Delta G_{Ca,1}$ is actually more favorable for Bet v 4 than for Bra n 1 and Phl p 7.

The N-terminal four residues are relatively disordered in the solution structure of Ca^{2+}-bound Bet v 4. If the N-terminal extension were to participate in noncovalent contacts with the polcalcin core sequence in the apo form, then Ca^{2+} binding would require disruption of those contacts: enthalpically unfavorable, entropically favorable. A similar scenario might likewise operate in Bra n 2.

Although Bet v 4, Bra n 1, Bra n 2, and Phl p 7 have qualitatively similar effects on ANS fluorescence, there are some quantitative differences. In each case, addition of the Ca^{2+}-bound protein to a dilute ANS solution substantially raises the quantum yield. Interestingly, the increase in ANS emission observed with Bra n 2 exceeds that observed with either Bet v 4, Bra n 1, or Phl p 7 by a factor of 3. This finding suggests that Bra n 2 has higher affinity for the fluorescent probe. The binding of ANS to proteins can involve both hydrophobic and electrostatic components (*36*−*39*). Whereas the naphthyl ring can associate with solvent-accessible apolar surface, the sulfonate group can interact with cationic side chains. *A priori*, it is possible that Bra n 2 exposes more apolar surface in the Ca^{2+}-bound state than Bet v 4, Bra n 1, or Phl p 7. Alternatively, the Bra n 2 sequence may harbor a strategically placed cationic side chain, with which the ANS sulfonate can interact. However, based on inspection of the sequences of the other three proteins (Figure 1), there do not appear to be any lysyl or arginyl side chains unique to Bra n 2. H36 is a potential candidate (proline or alanine occupy the corresponding position in the other three proteins) provided that the pK_a of the imidazolium side chain is shifted upward by interaction with the sulfonate. However, H36 is not immediately adjacent to the presumptive site of ANS association, a hydrophobic groove exposed upon Ca^{2+} binding (*30*). Thus, at present, the basis for the greater impact of Ca^{2+}-bound Bra n 2 on ANS emission is unclear. The apo- and Mg^{2+}-bound forms of all four proteins have a smaller impact on ANS fluorescence. In the case of Bra n 1, Bra n 2, and Phl p 7, the increase in emission is negligible. However, addition of apo- or Mg^{2+}-bound Bet v 4 to an ANS solution produces an increase in fluorescence roughly one-third of that seen with the Ca^{2+}-bound protein.

Our previous study of Phl p 7 noted the disparate conformational stabilities of Phl p 7 and Bet v 4. At the time, we did not know whether the stability of Bet v 4 was an anomaly. Having now examined the thermal stabilities of Bet v 4 and two additional polcalcin isoforms in some detail, it would appear that the thermal stability of Bet v 4 is the more representative and that Phl p 7 is, in fact, the outlier. The Ca^{2+}-free forms of Bet v 4, Bra n 1, and Bra n 2 possess free energies for unfolding of 3.1 ± 0.2, 3.2 ± 0.2, and 3.9 ± 0.2 kcal mol^{-1}, respectively. By contrast, the corresponding values for Phl p 7 and Phl p 7 D55S are 6.4 ± 0.3 and 6.9 ± 0.4 kcal mol^{-1}, respectively. The stability parameters exhibit little correlation with N-terminal extension length. Although it is true that the two proteins with the longer sequences, Bet v 4 and Bra n 2, have T_m values lower than that of Bra n 1, the T_m of the latter is still 21° lower than that of Phl p 7. Evidently, the explanation for the enhanced conformational stability of Phl p 7 must be found elsewhere.

The most glaring difference in the thermal stability parameters for Phl p 7 is seen in the denaturational heat capacity increment, ΔC_p. Bet v 4, Bra n 1, and Bra n 2 exhibit values of 0.66 ± 0.11, 0.95 ± 0.08, and 0.95 ± 0.07 kcal mol^{-1} K^{-1}, respectively. By contrast, the ΔC_p values determined for Phl p 7 and Phl p 7 D55S are 0.34 ± 0.03 and 0.32 ± 0.08 kcal mol^{-1} K^{-1}, respectively. Assuming that the magnitude of ΔC_p scales with the change in solvent-accessible apolar surface, this result suggests that unfolding of Phl p 7 is accompanied by substantially less exposure of hydrophobic surface, relative to the other three proteins. Employing the scaling factors suggested by Xie and Freire (*40*) for relating exposed surface area to ΔC_p, we estimate that thermal denaturation of Bet v 4 is accompanied by exposure of 2750 ± 310 $Å^2$ of apolar surface. By contrast, unfolding of either Phl p 7 or Phl p 7 D55S results in exposure of just 1900 ± 100 $Å^2$ of apolar surface.

Figure 1B compares the sequences of Bet v 4 and Phl p 7, with regions depicted in black indicating identity and residues depicted in gray indicating conservative substitutions. Evidently, the discrepancy in the ΔC_p values does not arise from major differences in apolar residue composition. Furthermore, the absence of correlation among the ΔC_p values for Bet v 4, Bra n 1, and Bra n 2 implies that the N-terminal extension is not a major contributing factor.

Increased electrostatic repulsion in Phl p 7 could produce an expansion of the native Ca^{2+}-free form, and the resulting increase in solvent penetration might explain the reduced ΔC_p value. The predicted isoelectric point of Phl p 7, at 3.98, is somewhat lower than those of Bet v 4 (4.57), Bra n 1 (4.29), and Bra n 2 (4.50). However, this difference does not translate into a large difference in net charge. Whereas the latter three proteins are predicted to have net charges at pH 7.5, in the Ca^{2+}-free state, of −6.0, −7.0, and −6.0, respectively, the predicted charge for Phl p 7 is only slightly higher, at −8.1. Significantly, elimination of a negative charge in the latter, via the D55S mutation, causes very minimal perturbation of ΔC_p.

An alternative explanation for the reduced ΔC_p value is the retention of residual structure in the unfolded state. It has been suggested that the enhanced thermal stability displayed by proteins from thermophilic organisms derives in part from a reduction in the denaturational heat capacity increment (*41*, *42*), which has the effect of lowering and, more importantly, broadening the protein stability curve. Relative to the enzyme from the mesophile *E. coli*, RNase H from the thermophile *Thermus aquaticus* has a substantially higher T_m and substantially smaller ΔC_p for unfolding: 86 vs 66 °C and 1.8 vs 2.7 kcal mol^{-1} K^{-1}, respectively. Robic et al. (*43*) presented evidence that the diminished heat capacity change reflects the retention of residual structure in the unfolded thermophilic protein. NMR studies have shown that native-like structure and topology can be retained in the unfolded state, even at high denaturant concentrations (*44*, *45*). Perhaps the atypically low ΔC_p that we observe for Phl p 7 has a similar origin. If so, the diminutive size of the protein would make it an attractive model system for exploring the sequence dependence of this phenomenon.

Concluding Remarks. Whereas the polcalcin EF-hand 2 consensus sequence includes four anionic ligands, the Phl p 7 site 2 harbors five. This pentacarboxylate site exhibits superior divalent ion affinity in engineered variants of rat α- and β-parvalbumins. By contrast, the divalent ion-binding signature of Phl p 7 is singularly unremarkable, as judged by comparison with three other polcalcin isoforms (Bet v 4, Bra n 1, and Bra n 2). In fact, if D55 in Phl p 7, which occupies the $-x$ position of site 2, is replaced with the consensus residue serine, the affinity for Ca^{2+} increases. This behavior, in direct conflict with that observed in

the parvalbumin background, may be a reflection of the allosteric nature of Ca^{2+} binding in the polcalcin system.

Phl p 7 exhibits anomalously high thermal stability when compared to the other three polcalcin isoforms. The heightened stability is apparently the consequence of an atypically small ΔC_p value. Inspection of the primary structures of Phl p 7 and the other three isoforms reveals no obvious origin for the diminutive ΔC_p. We suggest that it is a consequence of residual ordered structure in the denatured ensemble.

REFERENCES

1. Engel, E., Richter, K., Obermeyer, G., Briza, P., Kungl, A. J., Simon, B., Auer, M., Ebner, C., Rheinberger, H. J., Breitenbach, M., and Ferreira, F. (1997) Immunological and biological properties of Bet v 4, a novel birch pollen allergen with two EF-hand calcium-binding domains. *J. Biol. Chem. 272*, 28630–28637.
2. Ledesma, A., Villalba, M., Batanero, E., and Rodriguez, R. (1998) Molecular cloning and expression of active Ole e 3, a major allergen from olive-tree pollen and member of a novel family of Ca^{2+}-binding proteins (polcalcins) involved in allergy. *Eur. J. Biochem. 258*, 454–459.
3. Rozwadowski, K., Zhao, R., Jackman, L., Huebert, T., Burkhart, W. E., Hemmingsen, S. M., Greenwood, J., and Rothstein, S. J. (1999) Characterization and immunolocalization of a cytosolic calcium-binding protein from *Brassica napus* and *Arabidopsis* pollen. *Plant Phys. 120*, 787–798.
4. Suphioglu, C., Ferreira, F., and Knox, R. B. (1997) Molecular cloning and immunological characterisation of Cyn d 7, a novel calcium-binding allergen from Bermuda grass pollen. *FEBS Lett. 402*, 167–172.
5. Okada, T., Zhang, Z., Russell, S. D., and Toriyama, K. (1999) Localization of the Ca^{2+}-binding protein, Bra r 1, in anthers and pollen tubes. *Plant Cell Physiol. 40*, 1243–1252.
6. Hayek, B., Vangelista, L., Pastore, A., Sperr, W. R., Valent, P., Vrtala, S., Niederberger, V., Twardosz, A., Kraft, D., and Valenta, R. (1998) Molecular and immunologic characterization of a highly cross-reactive two EF-hand calcium-binding alder pollen allergen, Aln g 4: structural basis for calcium-modulated IgE recognition. *J. Immunol. 161*, 7031–7039.
7. Niederberger, V., Hayek, B., Vrtala, S., Laffer, S., Twardosz, A., Vangelista, L., Sperr, W. R., Valent, P., Rumpold, H., Kraft, D., Ehrenberger, K., Valenta, R., and Spitzauer, S. (1999) Calcium-dependent immunoglobulin E recognition of the apo- and calcium-bound form of a cross-reactive two EF-hand timothy grass pollen allergen, Phl p 7. *FASEB J. 13*, 843–856.
8. Twardosz, A., Hayek, B., Seiberler, S., Vangelista, L., Elfman, L., Gronlund, H., Kraft, D., and Valenta, R. (1997) Molecular characterization, expression in *Escherichia coli*, and epitope analysis of a two EF-hand calcium-binding birch pollen allergen, Bet v 4. *Biochem. Biophys. Res. Commun. 239*, 197–204.
9. Celio, M. R., Pauls, T., and Schwaller, B. (1996) Guidebook to the Calcium-Binding Proteins, Oxford University Press, New York.
10. Kretsinger, R. H. (1980) Structure and evolution of calcium-modulated proteins. *CRC Crit. Rev. Biochem. 8*, 119–174.
11. Kawasaki, H., and Kretsinger, R. H. (1995) Calcium-binding proteins 1: EF-hands. *Protein Profile 2*, 297–490.
12. Kretsinger, R. H., and Nockolds, C. E. (1973) Carp muscle calcium-binding protein. II. Structure determination and general description. *J. Biol. Chem. 248*, 3313–3326.
13. McPhalen, C. A., Strynadka, N. C. J., and James, M. N. G. (1991) Calcium-binding sites in proteins: a structural perspective. *Adv. Protein Chem. 42*, 77–144.
14. Henzl, M. T., Davis, M. E., and Tan, A. (2008) Divalent ion binding properties of the timothy grass allergen, Phl p 7. *Biochemistry 47*, 7846–7856.
15. Henzl, M. T., Hapak, R. C., and Goodpasture, E. A. (1996) Introduction of a fifth carboxylate ligand heightens the affinity of the oncomodulin CD and EF sites for Ca^{2+}. *Biochemistry 35*, 5856–5869.
16. Henzl, M. T., Agah, S., and Larson, J. D. (2004) Rat α- and β-parvalbumins: comparison of their pentacarboxylate and site-interconversion variants. *Biochemistry 43*, 9307–9319.
17. Weber, G., and Young, L. (1964) Fragmentation of bovine serum albumin by pepsin. I. The origin of the acid expansion of the albumin molecule. *J. Biol. Chem. 239*, 1415–1423.
18. Warren, J. R., and Gordon, J. A. (1966) On the refractive indices of aqueous solutions of urea. *J. Phys. Chem. 70*, 297–300.
19. Perkins, S. J. (1986) Protein volumes and hydration effects: the calculations of partial specific volumes, neutron scattering matchpoints and 280-nm absorption coefficients for proteins and glycoproteins from amino acid sequences. *Eur. J. Biochem. 157*, 169–180.
20. Haner, M., Henzl, M. T., Raissouni, B., and Birnbaum, E. R. (1984) Synthesis of a new chelating gel: removal of Ca^{2+} ions from parvalbumin. *Anal. Biochem. 138*, 229–234.
21. Henzl, M. T., Agah, S., and Larson, J. D. (2003) Characterization of the metal ion-binding domains from rat α- and β-parvalbumins. *Biochemistry 42*, 3594–3607.
22. Bevington, P. R., and Robinson, D. K. (1992) Data Reduction and Error Analysis for the Physical Sciences, 2nd ed., McGraw-Hill, Boston, MA.
23. Henzl, M. T., Larson, J. D., and Agah, S. (2003) Estimation of parvalbumin Ca^{2+}- and Mg^{2+}-binding constants by global least-squares analysis of isothermal titration calorimetry data. *Anal. Biochem. 319*, 216–233.
24. Henzl, M. T., Larson, J. D., and Agah, S. (2004) Influence of monovalent cation identity on parvalbumin divalent ion-binding properties. *Biochemistry 43*, 2747–2763.
25. Henzl, M. T. (2009) Characterization of parvalbumin and polcalcin divalent ion binding by isothermal titration calorimetry. *Methods Enzymol. 455*, 259–296.
26. Henzl, M. T., and Ndubuka, K. (2007) Low-affinity signature of the rat β-parvalbumin CD site. Evidence for remote determinants. *Biochemistry 46*, 23–35.
27. Pace, C. N., and Laurents, D. V. (1989) A new method for determining the heat capacity change for protein folding. *Biochemistry 28*, 2520–2525.
28. McCrary, B. S., Edmondson, S. P., and Shriver, J. W. (1996) Hyperthermophile protein folding thermodynamics: differential scanning calorimetry and chemical denaturation of Sac7d. *J. Mol. Biol. 264*, 784–805.
29. Santoro, M. M., and Bolen, D. W. (1988) Unfolding free energy changes determined by the linear extrapolation method. 1. Unfolding of phenylmethanesulfonyl α-chymotrypsin using different denaturants. *Biochemistry 27*, 8063–8068.
30. Neudecker, P., Nerkamp, J., Eisenmann, A., Nourse, A., Lauber, T., Schweimer, K., Lehmann, K., Schwarzinger, S., Ferreira, F., and Rosch, P. (2004) Solution structure, dynamics, and hydrodynamics of the calcium-bound cross-reactive birch pollen allergen Bet v 4 reveal a canonical monomeric two EF-hand assembly with a regulatory function. *J. Mol. Biol. 336*, 1141–1157.
31. Verdino, P., Westritschnig, K., Valenta, R., and Keller, W. (2002) The cross-reactive calcium-binding pollen allergen, Phl p 7, reveals a novel dimer assembly. *EMBO J. 21*, 5007–5016.
32. Lee, Y. H., Tanner, J. J., Larson, J. D., and Henzl, M. T. (2004) Crystal structure of a high-affinity variant of rat α-parvalbumin. *Biochemistry 43*, 10008–10017.
33. Reid, R. E., and Hodges, R. S. (1980) Co-operativity and calcium/magnesium binding to troponin C and muscle calcium binding parvalbumin: an hypothesis. *J. Theor. Biol. 84*, 401–444.
34. Reid, R. E. (1990) Synthetic fragments of calmodulin calcium-binding site III. A test for the acid-pair hypothesis. *J. Biol. Chem. 265*, 5971–5976.
35. Procyshyn, R. M., and Reid, R. E. (1994) A structure/activity study of calcium affinity and selectivity using a synthetic peptide model of the helix-loop-helix calcium-binding motif. *J. Biol. Chem. 269*, 1641–1647.
36. Matulis, D., and Lovrien, R. (1998) 1-Anilino-8-naphthalene sulfonate anion-protein binding depends primarily on ion pair formation. *Biophys. J. 74*, 422–429.
37. Ory, J. J., and Banaszak, L. J. (1999) Studies of the ligand binding reaction of adipocyte lipid binding protein using the fluorescent probe 1-anilinonaphthalene-8-sulfonate. *Biophys. J. 77*, 1107–1116.
38. Schonbrunn, E., Eschenburg, S., Luger, K., Kabsch, W., and Amrhein, N. (2000) Structural basis for the interaction of the fluorescence probe 8-anilino-1-naphthalene sulfonate (ANS) with the antibiotic target MurA. *Proc. Natl. Acad. Sci. U.S.A. 97*, 6345–6349.
39. Lartigue, A., Gruez, A., Spinelli, S., Riviere, R., Brossut, R., Tegoni, M., and Cambillau, C. (2003) The crystal structure of a cockroach pheromone-binding protein suggests a new binding and release mechanism. *J. Biol. Chem. 278*, 30213–30218.
40. Xie, D., and Freire, E. (1994) Structure based prediction of protein folding intermediates. *J. Mol. Biol. 242*, 62–80.
41. Hollien, J., and Marqusee, S. (1999) A thermodynamic comparison of mesophilic and thermophilic ribonucleases H. *Biochemistry 38*, 3831–3836.

42. Deutschman, W. A., and Dahlquist, F. W. (2001) Thermodynamic basis for the increased thermostability of CheY from the hyperthermophile *Thermotoga maritima*. *Biochemistry 40*, 13107–13113.
43. Robic, S., Guzman-Casado, M., Sanchez-Ruiz, J. M., and Marqusee, S. (2003) Role of residual structure in the unfolded state of a thermophilic protein. *Proc. Natl. Acad. Sci. U.S.A. 100*, 11345–11349.
44. Shortle, D., and Ackerman, M. S. (2001) Persistence of native-like topology in a denatured protein in 8 M urea. *Science 293*, 487–489.
45. Klein-Seetharaman, J., Oikawa, J., Grimshaw, S. B., Wirmer, J., Duchardt, E., Ueda, T., Imoto, T., Smith, L. J., Dobson, C. M., and Schwalbe, H. (2002) Long-range interactions within a nonnative protein. *Science 295*, 1719–1722.